Advances in Science and Technology Research Journal

Advances in Science and Technology Research Journal, 2026, 20(9), 259–269
https://doi.org/10.12913/22998624/222685
ISSN 2299-8624, License CC-BY 4.0

Received: 2026.05.06
Accepted: 2026.07.10
Published: 2026.08.01

A unified methodology for determination of the formability characteristics by plastometric torsion test

Jacek Pawlicki[1*], Adam Płachta[2], Szymon Pawlak[2*]

[1] Faculty of Transport and Aviation Engineering, Silesian University of Technology, Krasińskiego 8, 40-019 Katowice, Poland
[2] Faculty of Materials Engineering and Digitalization Industrial, Silesian University of Technology, Krasińskiego 8, 40-019 Katowice, Poland
* Corresponding author's e-mail: szymon.pawlak@polsl.pl

ABSTRACT

The paper presents a unified procedure for determining the characteristics of technological plasticity of materials in a torsion test, ensuring repeatability and reproducibility of experimental results. The description of the procedure is preceded by an analysis of research results obtained independently at two research centers: TU Bergakademie Freiberg and Silesian University of Technology. The experiments were conducted on specimens made of austenitic steel 0H18N9 (1.4301), maintaining identical test parameters, namely strain rate and temperature. The remaining test conditions reflected the specific characteristics of the equipment and specimen geometries used at each research center. The analysis of plastometric test results indicates that at a temperature of 900 °C, the maximum flow stress values were obtained at the Silesian University of Technology. In the remaining temperature range, from 1000 °C to 1150 °C, the highest flow stress values (σp) were recorded at TU Bergakademie Freiberg. The highest values of limiting strains (εg and εp), across the entire temperature range, were obtained from the experiments conducted at the Silesian University of Technology. The obtained experimental results and the comparative analysis performed confirm the validity of developing a unified methodology for determining the characteristics of technological plasticity in torsion tests. The proposed methodology systematizes the experimental procedure, from the selection of specimen geometry to the acquisition of test results and the method of converting recorded measurement data. The paper presents a unified procedure for determination of the formability characteristics, which ensures good repeatability and reproducibility of results. A methodology for performing the experiment as well as a method for converting experimental data into the flow stress - strain relationship are suggested.

Keywords: torsion, flow stress, plastometric torsion test, flow curve.

INTRODUCTION

Accurate characterization of the technological plasticity of a material particularly the flow stress function is associated both with the mathematical form of the function and the methodology used for the experimental determination of flow stress [1]. The form of the flow stress function determines the correctness of calculations of metal forming process parameters, the analysis of their course, as well as physical and numerical modeling. Flow stress (σ_p), alongside the limiting strain (ε_g), is a fundamental parameter characterizing the material's susceptibility to plastic deformation. The general formulation describing flow stress defined as the stress required to initiate and sustain plastic flow of a material is a function of strain (ε), strain rate ($\dot{\varepsilon}$), temperature (T), and the history of deformation (h_ε):

$$\sigma_p = \sigma_p(\varepsilon, \dot{\varepsilon}, T, h_\varepsilon) \quad (1)$$

In cold metal forming processes, the flow stress is a function of the strain magnitude (ε) and the deformation history h_ε:

$$\sigma_p = \sigma_p(\varepsilon, h_\varepsilon) \quad (2)$$

The parameters describing the deformation history include: the magnitude of a single strain increment and the strain path, defined by

the evolution of strain components as a function of time, as well as the time intervals between successive deformation steps. For deformation states described by principal strains, it is necessary to know the orientation of the principal axes and the values of the principal strain components as functions of time:

$$\varepsilon_1 = \varepsilon_1(t),\ \varepsilon_2 = \varepsilon_2(t), \varepsilon_3 = \varepsilon_3(t) \qquad (3)$$

The deformation history should be understood as the course of deformation as a function of all process parameters that determine material hardening and softening. If the analysis is limited to the three primary parameters, namely strain (ε), strain rate ($\dot{\varepsilon}$), and temperature (T), the deformation path can be represented in a three-dimensional space (Figure 1). The two deformation paths a and b shown in the figure intersect at a single point B, which means that at this point the values of ε, $\dot{\varepsilon}$, and T are identical for both paths. Despite this, the values of flow stress at point B for the two paths may differ. This indicates the influence of deformation history on flow stress. Therefore, flow stress cannot be treated as a function of only three variables ε, $\dot{\varepsilon}$, and T. Such a function would not be unambiguous [2].

The most commonly used methods for assessing technological plasticity include tensile, compression, and torsion tests, as well as model upsetting and rolling tests. Methods for determining the characteristics of technological plasticity of materials are continuously evolving. In the study of metallic materials, commercially available thermo-mechanical processing simulators, considered to be technologically advanced, are now widely used, such as the Gleeble 3800 system and the MaxStrain device operating in conjunction with this system [3–6].

The Gleeble 3800 thermo-mechanical simulator enables the performance of an axisymmetric compression test. The unique design of the measuring head, combined with the use of two independent hydraulic systems, allows the elimination of acceleration and deceleration phases of the forming tool during specimen deformation. An additional advantage of this test is the ability to obtain accurate values of both incremental and total strains at high strain rates. A significant limitation of axisymmetric deformation testing, however, is the relatively low achievable strain. For a standard cylindrical specimen with dimensions of φ10 × 15 mm compressed using the Gleeble simulator, the strain value generally does not exceed 1.2. The MaxStrain method enables the simulation of thermo-mechanical processing with a cyclic change in the deformation path, achieved by rotating the specimen by 90° between successive deformation steps, with either free or fixed specimen ends (Figure 2a). The accumulated plastic strain can reach a value of approximately 20 (equivalent strain). An advantage of this device is the precise control of strain and strain rate, as well as the possibility of combining plastic deformation with heat treatment [7–9]. The loading method applied during deformation, involving a 90° rotation of the specimen between successive steps, leads to the formation of intensely plastically deformed zones in the specimen cross-section. These zones take the form of intersecting regions in which the material flows toward the upper and lower surfaces of the specimen (Figure 2b). The shape of these regions remains unchanged in subsequent deformation cycles. In the remaining regions, which are in direct contact with the tool surfaces (upper and lower anvils) and adjacent to the free surfaces of the specimen, the strain values are significantly lower. The high non-uniformity of strain distribution across the specimen cross-section necessitates the selection of a representative area for structural analysis. Accurate determination of local strain values is possible only with the use of finite element method (FEM) simulations.

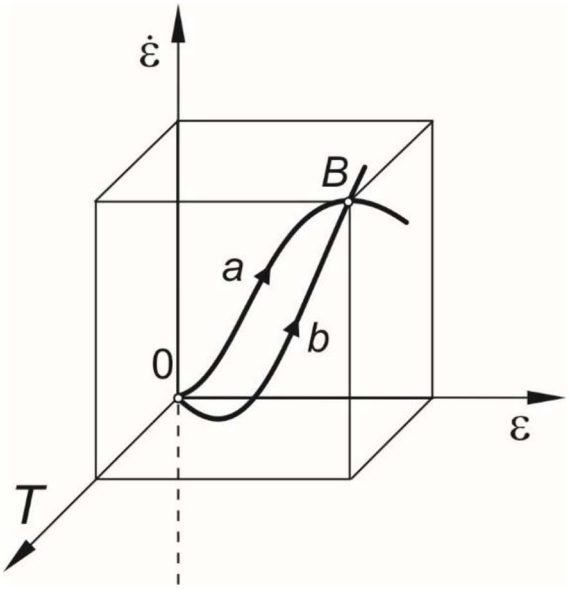

Figure 1. Diagram representing courses of two different forming processes resulting in the same values of process parameters: ε, $\dot{\varepsilon}$ and *T* at point *B* [2]

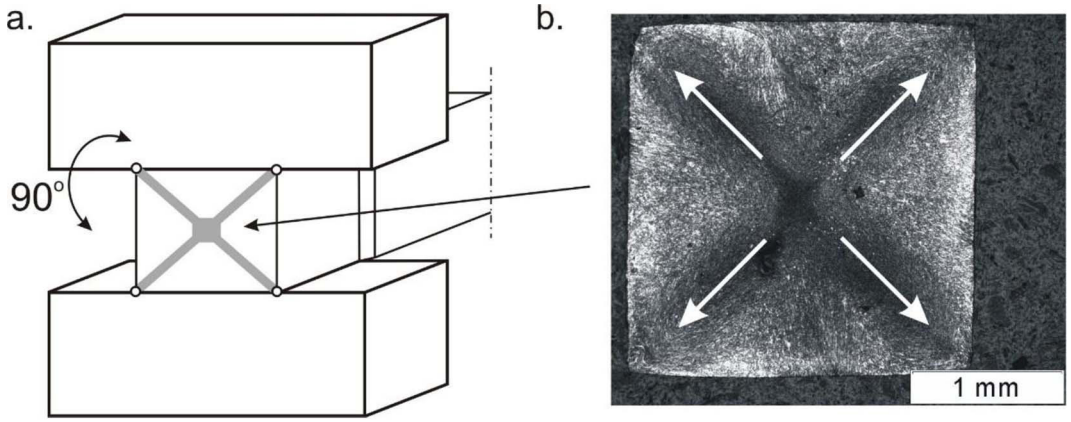

Figure 2. Deformation by means of the MaxStrain simulator (a), and macrostructure on the metallographic cross–section of a copper sample after deformation in the simulator: equivalent strain ε_i = 8,6, the arrows indicate the direction of material flow in the most intensely deformed areas (b)

A distinguishing feature of the torsion test is the time-invariant stress state. It corresponds, with high accuracy, to pure shear in the initial stage of deformation and enables the achievement of large permanent strains, significantly greater than those obtained in tensile and compression tests, without prior loss of stability. However, the lack of standardization for plastometric torsion testing has led individual research centers to develop their own procedures for conducting such experiments [10–14]. The use of different specimen geometries, calibration of measurement sensors, variations in experimental procedures, and different methods of converting measured values into strain–flow stress relationships have resulted in the inability to directly compare results obtained at different research centers.

Many factors significantly influence the obtained test results. These include, among others, the thermal effect associated with plastic deformation work and the resulting temperature gradients along the length and across the cross-section of the specimen, the degree of strain localization, specimen geometry, the method of specimen fixation, as well as the non-uniformity of strain distribution along the length and across the cross-section. This non-uniformity makes it difficult to determine the exact value of local strain in the observed region and necessitates the development of a methodology for selecting locations for structural analysis.

The plastometric torsion test has considerable potential for the investigation of steels, non-ferrous metal alloys, and sintered materials under a wide range of deformation and temperature conditions [15–18]. A methodologically distinctive approach is the use of a torsion plastometer for studying metal plasticity under conditions of a variable deformation path. However, this requires additional modifications to the plastometer design in order to introduce supplementary loading, such as axial force, or a cyclically varying torsional moment [19].

All the above arguments justify the need to develop a standard for plastometric torsion testing, which would systematize experimental procedures, from the selection of specimen geometry, through the research methodology, to unified algorithms for converting recorded measurement signals into flow stress and strain values. The developed algorithms should eliminate effects associated with discrepancies between imposed and achieved test parameters. The results obtained using a universal procedure defined in such a standard would enable direct comparison of data generated in different research centers. Moreover, the determined flow stress values, as intrinsic material properties, would allow accurate characterization of technological plasticity. This paper presents a proposal for a unified methodology for determining the characteristics of technological plasticity in the torsion test.

PLASTOMETRIC TESTING IN THE TORSION TEST

Based on the authors' experience and the methodological nature of this study, austenitic steel 0H18N9 (1.4301) was selected as the test material. Within the investigated range of deformation parameters (900–1150 °C), the

steel exhibits a stable single-phase austenitic structure. The material used for the experiments consisted of hot-rolled bars made of Cr–Ni austenitic steel, the chemical composition of which is presented in Table 1.

To eliminate the effect of initial microstructural variability on the test results, the specimens were subjected to heat treatment prior to torsion. The treatment consisted of solution annealing at 1150 °C, with a holding time of 1 hour, followed by water quenching. The heat treatment was carried out in a silite electric furnace manufactured by Carbolite Gero, with a temperature control accuracy of ±5 °C. The applied heat treatment ensured the dissolution of carbide precipitates and the attainment of a microstructure with a minimal grain size. The prepared specimens were subsequently transferred to TU Bergakademie Freiberg (Institut für Metallformung) to perform experiments according to the joint program presented in Table 2 and to compare the obtained results, both at the level of recorded measurement signals and the resulting flow curves, with those obtained at the Silesian University of Technology.

RESULTS

Figure 3 presents an exemplary comparison of the recorded measurement data in the form of torque–shear strain relationships obtained at the research centers. The data were subjected only to basic processing consisting of filtering the recorded measurement points in order to eliminate errors arising during data acquisition. The comparative studies carried out at both centers revealed differences in the obtained values already at the level of the recorded measurement data. These discrepancies result from the use of specimens with different geometrical characteristics, as well as from differences in the heating methods applied. At TU Bergakademie Freiberg, specimens with a gauge length of L = 15 mm and a diameter of d = 6 mm are heated in a silite furnace, whereas at the Silesian University of Technology, specimens with a gauge length of L = 50 mm and a diameter of d = 6 mm are heated inductively.

A review of the literature indicates that plastometric investigations employ specimens with diameters ranging from 6 to 10 mm and slenderness ratios, expressed as the ratio of gauge length to diameter (L/d), varying from 1/3 to 10. Variations in specimen slenderness primarily result from the need to increase the strain rate. In Poland, the most commonly used specimens have a diameter of d = 6 mm and lengths of L = 50 mm or 10 mm, based on the specimen geometry applied in IRSID-France studies. At the maximum rotational speed of 1000 rpm typically used in torsion plastometers, a specimen with a gauge length of L = 50 mm enables the achievement of a strain rate of $\dot{\varepsilon} = 3.6\ s^{-1}$. Reducing the gauge length to L = 10 mm increases the strain rate to $\dot{\varepsilon} = 18.2\ s^{-1}$. According to the studies conducted by Funke and Preiser, both the shape of the flow curves and the flow stress values determined from the recorded torque measurements vary with changes in gauge length [20]. Nevertheless, the studies demonstrated that the most stable and repeatable results were obtained for specimen diameters ranging from 6 to 9 mm and slenderness ratios between 1/3 and 10. These criteria are satisfied by the most commonly used specimens with a diameter of d = 6 mm and lengths of L = 50 mm and L = 10 mm. It should be emphasized that during a given experimental series, the specimen geometry remains unchanged.

The various specimen heating methods applied in the presented plastometer designs arise from prior experience in hot metal plasticity testing, the technical capabilities available to individual

Table 2. Joint research program

T, °C	Strain rate, s^{-1}		
	0.036	0.36	3.6
900	x	x	x
1000	x	x	x
1050	x	x	x
1100	x	x	x
1150	x	x	x

Table 1. Chemical composition of 0H18N9 steel (1.4301)

Element content, % by mass					
C	Cr	Mn	Ni	P	S
0.028	18.40	0.187	8.90	0.036	0.012

research teams for constructing experimental setups, and differing experimental requirements. Heating in a silicon carbide resistance furnace is a relatively slow process resulting from heat conduction from the heating elements to the specimen material. In induction furnaces, heat is generated directly within the material through the induction of eddy currents, which ensures rapid heating of the specimen. However, induction heating is considerably more difficult for materials characterized by low electrical resistivity. These limitations do not apply to furnaces equipped with silicon carbide heating elements. In this study, it was assumed that both silicon carbide furnace heating and induction heating ensure the achievement of the required stable material temperature throughout the duration of the test. If the experimental procedure is carried out at a prescribed and constant temperature, the obtained flow stress values, being intrinsic material properties, should remain identical regardless of the heating technique employed.

The conversion of recorded measurement data into the flow stress–strain relationship was carried out at both research centers using their respective calculation procedures. At TU Bergakademie Freiberg, the measurement signals from sensors are recorded in a text file. During the test, the following quantities are registered: axial force F (N), angle of twist (deg), and torque M (Nm), all as functions of time t (s). The recorded data are subsequently processed using the AUK software. It should be noted that during the plastometric torsion test, the instantaneous temperature is not recorded, as the specimen is heated in a silite furnace preheated to the deformation temperature. Corrections to the flow stress values with respect to temperature are performed under the assumption that a portion of the plastic deformation work is converted into heat, according to the following relationship (4):

$$\Delta T = \frac{\sigma_p \varepsilon}{\rho c} \tag{4}$$

where: σ_p – flow stress, ε – strain, ρ – density, c – specific heat capacity.

It is assumed that for relatively low strain rates of approximately 0.04 s^{-1}, about 30% of the plastic deformation work calculated from Equation 4 is converted into heat, whereas for high strain rates of approximately 4 s^{-1} and above, this fraction reaches about 90%. Therefore, this correction is approximate and not based on the actual temperature increase of the specimen during torsion. The correction for strain rate and temperature is carried out within the computational module of the AUK software, using flow stress values.

At TU Bergakademie Freiberg, specimens with a gauge length of L = 15 mm are used. The values of strain and flow stress are determined from the following relationships:

$$\varepsilon = \frac{2}{\sqrt{3}} arcsin\, h\left(\frac{\pi \bar{R} N}{L}\right) \tag{5}$$

where: $\bar{R} = \frac{3}{4}R$

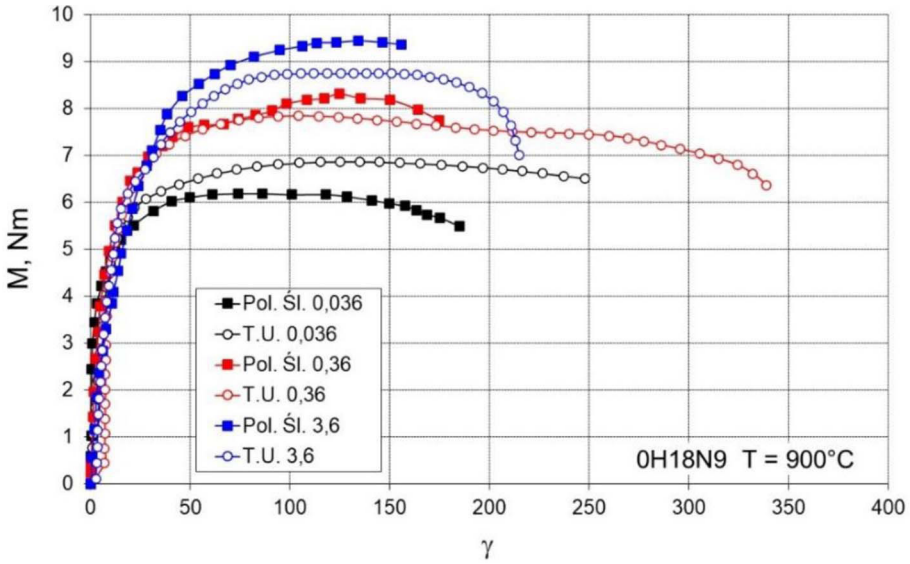

Figure 3. The torque – non-dilatational strain relationship, obtained for various strain rates in the various research centers (Pol. Śl. – Silesian University of Technology, T. U. – TU Bergakademie Freiberg)

$$\sigma_p = \sqrt{3\tau^2 + \sigma_L^2} \tag{6}$$

where: $\tau = \frac{3M}{\pi \bar{R}^3}$, $\sigma_L = \frac{F_L}{\pi \bar{R}^2}$

Thus, at TU Bergakademie Freiberg, the parameters p (strain hardening) and m (strain rate sensitivity) are neglected in the calculation of flow stress, and only the stress resulting from the applied axial force is considered. At the Silesian University of Technology, specimens with a gauge length of L = 50 mm are used, and strain is determined for an equivalent radius of $\bar{R} = \frac{2}{3}R$. A representative comparison of the obtained flow curves at both research centers is presented in Figures 4 and 5. Analysis of the flow curves over the full range of deformation parameters shows that at a test temperature of 900 °C, the maximum flow stress values were obtained at the Silesian University of Technology (Figure 4), whereas in the remaining temperature range from 1000 °C to 1150 °C, the highest flow stress values (σp) were recorded at TU Bergakademie Freiberg (Figure 5). The highest values of limiting strains εg and εp (strain corresponding to the maximum flow

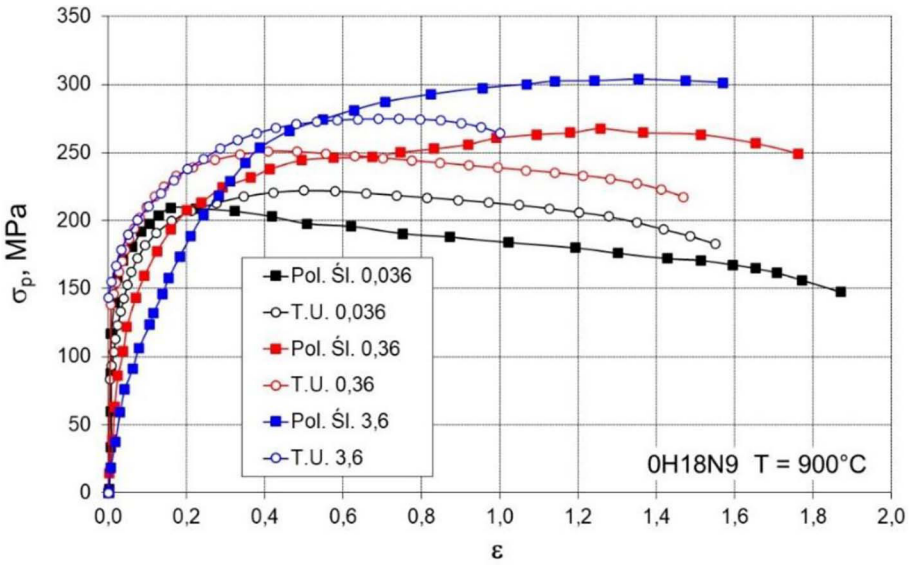

Figure 4. The flow stress curves, obtained for various strain rates in the various research centers (Pol Śl. – Silesian University of Technology, T. U. – TU Bergakademie Freiberg)

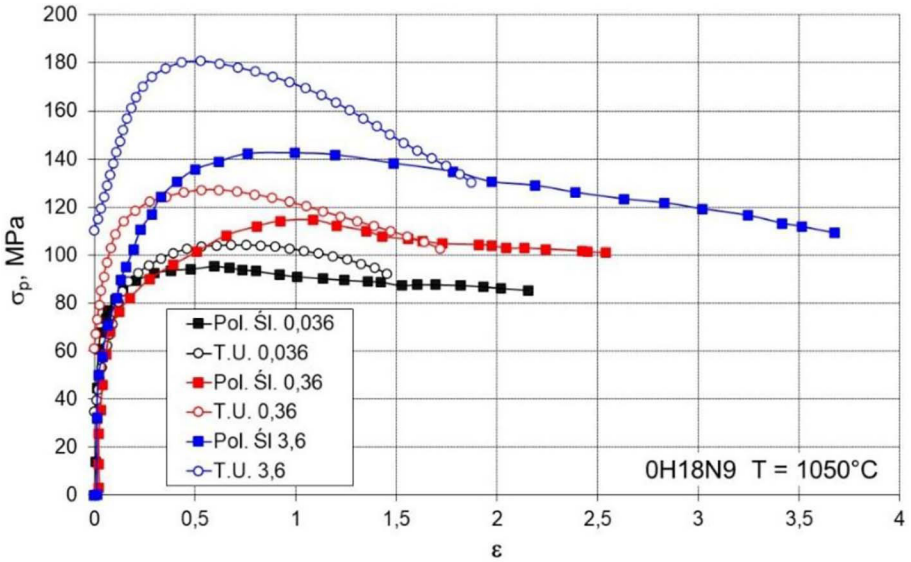

Figure 5. The flow stress curves, obtained for various strain rates in the various research centers (Pol Śl. – Silesian University of Technology, T. U. – TU Bergakademie Freiberg)

stress) across the entire temperature range were obtained for the results from the Silesian University of Technology. The lower values of limiting strain εg obtained at TU Bergakademie Freiberg result from the adoption of an equivalent radius $\bar{R} = \frac{3}{4}R$ for strain calculations. Within the investigated range of deformation parameters at the research centers, two characteristic types of torque–strain relationships and flow curves were observed. During hot torsion of steel at temperatures of 900 °C and 1000 °C, after exceeding the strain corresponding to the maximum flow stress, a gradual decrease in stress is observed until specimen failure. In specimens deformed at temperatures of 1050 °C and higher, for the entire analyzed range of strain rates, once the strain value ε_p is exceeded, the flow stress stabilizes at a constant level σ_{ps}. The steady-state flow stress σ_{ps} corresponds to the equilibrium between strain hardening and dynamic recrystallization. Differences in the results of plastometric tests conducted at various research centers arise from several factors, including:

- the design and level of technical advancement of torsion plastometers,
- variations in the selection of geometrical characteristics of plastometric specimens,
- differences in experimental procedures,
- methods used to convert measured data into flow stress and strain values,
- the influence of thermal effects and the methods used for their evaluation,
- the impact of non-uniform strain distribution along both the longitudinal and transverse cross-sections of the specimen.

Therefore, it appears necessary to standardize the procedure for plastometric torsion testing in order to enable comparison of results obtained at different research centers, both domestic and international.

UNIFIED METHODOLOGY FOR DETERMINING TECHNOLOGICAL PLASTICITY CHARACTERISTICS IN THE TORSION TEST

Before commencing the experimental investigation, the validity of calibration certificates for all measuring devices should be verified. The unified procedure for determining the characteristics of technological plasticity, developed at the Silesian University of Technology, consists of the following sequential stages.

Specimens for plastometric testing

Prior to the commencement of testing, it is necessary to perform quality control of the specimens. Specimens for plastometric tests should be manufactured in accordance with the technical drawings presented in Figure 6. Particular attention should be paid to the surface condition and the transition radii between the gripping section and the gauge section of the plastometric specimen.

Preparation and mounting of specimens

An essential step to be carried out before the actual experiment is the verification of specimen alignment. Alignment depends not only on the accuracy of specimen manufacturing but also on the method of fixing the specimen in the grips of the torsion plastometer heads. Alignment is checked using a double-pointed metal rod mounted in one of the plastometer heads.

Conditions of the torsion test

In the plastometer control program, appropriate test conditions should be defined in accordance with the experimental plan, including the required temperature and heating time, number of twists, and the method of specimen cooling. For sequential tests, the time intervals between successive deformation steps must also be specified. In order to approach the target values during parameter definition, the kinematic and dynamic characteristics of the mechanical system, as well as the thermal characteristics of the plastometer heating system, should be taken into account.

Recording and processing of measurement signals

The obtained experimental data are subjected to filtering, optional reduction (if the number of recorded data points is excessively high), truncation (to determine the limiting strain ε_g, corresponding to the number of twists to specimen failure), and smoothing using a moving average method or a higher-order polynomial. These operations are necessary to eliminate measurement errors and noise generated during the experimental procedure.

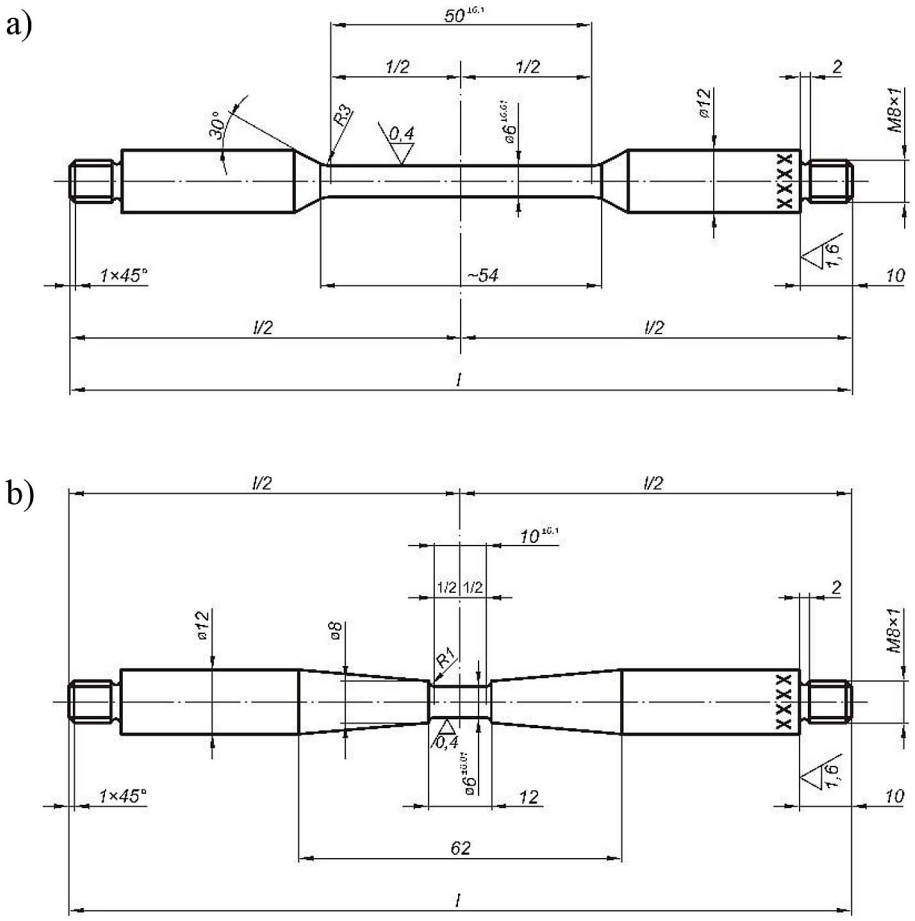

Figure 6. Samples used in the plastometric tests: (a) the standard sample with the gauge length L = 50 mm; (b) the short sample with the gauge length L = 10 mm (used for large strain rates)

Correction of torque with respect to variations in rotational speed M = f (N) ⇒ M′ = f (N)

In order to correct the torque with respect to rotational speed, Equation 7 is used:

$$M' = \left(\frac{\dot{N}}{\dot{N}_u}\right)^b M \tag{7}$$

where: $\dot{N}$ – imposed rotational speed, rpm; $\dot{N}_u$ – actual rotational speed, rpm; b – exponent of the function.

$$M = AN^B\, exp(CN)\, \dot{N}^{D+\frac{E}{T}}\, exp\left(\frac{F}{T}\right) \tag{8}$$

The constants A, B, C, D, E, and F appearing in Equation 10 are determined using multiple linear regression. The parameter b is calculated from Equation 9:

$$b = D + \frac{E}{T} \tag{9}$$

By correcting the torque values across the entire dataset according to Equation 7, a torque corrected for variations in rotational speed is obtained.

Correction of torque with respect to temperature variations during torsion M′ = f (N) ⇒ M″ = f (N)

The correction of torque with respect to temperature variations during torsion is calculated according to the following relationship.

$$M'' = M' + \Delta M \tag{10}$$

where:

$$\Delta M = AN^B\, exp(CN)\, \dot{N}^{D+\frac{E}{T}}\, exp\left(\frac{F}{T}\right) - AN^B\, exp(CN)\, \dot{N}^{D+\frac{E}{T+\Delta T}}\, exp\left(\frac{F}{T+\Delta T}\right) \tag{11}$$

Figure 7 presents the final result of correcting the torque values with respect to rotational speed and temperature variations.

Determination of parameters *p* and *m*

The parameter p is determined numerically by differentiating the relationship M″ = $f(N)$ for T = const and $\dot{\varepsilon}$ = const:

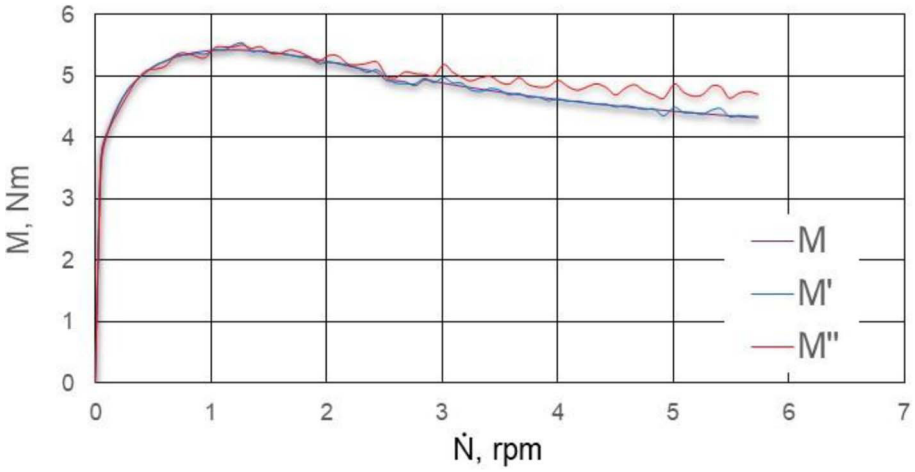

Figure 7. Final effect of torque correction due to the twist rate and temperature discrepancy T = 1000 °C, $\dot{N}$ = 100 rpm

$$p = \frac{N}{M''}\frac{\partial M''}{\partial N} = \frac{\frac{\partial M''}{M}}{\frac{\partial N}{N}} \approx \frac{\partial \ln M''}{\partial \ln N} = \frac{ln\big(M''(t+\Delta t)\big) - ln\big(M''(t)\big)}{ln\big(N(t+\Delta t)\big) - ln\big(N(t)\big)} \quad (12)$$

To determine the parameter *m*, the relationship ln M″ versus ln Ṅ should be plotted (for T = const and ε = const) for several values of the rotational speed Ṅ. The obtained data points are then approximated using the least squares method. The parameter *m* is calculated using Equation (13):

$$m = \frac{\dot{N}}{M''}\frac{\partial M''}{\partial \dot{N}} = \frac{\frac{\partial M''}{M''}}{\frac{\partial \dot{N}}{\dot{N}}} \approx \frac{\partial \ln M''}{\partial \ln \dot{N}} \quad (13)$$

Calculation of strain and flow stress

Strain is determined from the following relationship:

$$\varepsilon = \frac{1}{\sqrt{3}}\gamma = \frac{1}{\sqrt{3}}\frac{2\pi \cdot R \cdot N}{L} \quad (14)$$

Flow stress is determined from the following relationship:

$$\sigma_p = \sqrt{\left(\frac{\sqrt{3}M''}{2\pi R^3}\right)^2 (3+p+m)^2 + \left(\frac{F}{\pi R^2}\right)^2} \quad (15)$$

Correction of strain with respect to strain non-uniformity ($\varepsilon_{max} = \varepsilon_\delta$)

The strain non-uniformity coefficient δ was determined from the measurement of the inclination angle of a marker line applied to the plastometric specimen, as a function of temperature and rotational speed. The relationship δ = δ(T, Ṅ) was obtained by approximating the measured values.

$$\delta = A\dot{N}^B \, exp\left(\frac{C}{T}\right) \quad (16)$$

Determination of flow curves σp = f(ε) and the flow stress function σp = f(ε, $\dot{\varepsilon}$, T)

For the description of the flow stress function, the Hensel–Spittel equation or its modified form (17) should be used:

$$\sigma = A\varepsilon^B \, exp(C\varepsilon)\, \dot{\varepsilon}^{D+\frac{E}{T}} exp\left(\frac{F}{T}\right) \quad (17)$$

The constants A, B, C, D, E, and F appearing in Equation 17 are determined using multiple linear regression. A tabular representation of data describing the flow stress is also a highly effective method for characterizing the technological plasticity of materials, particularly for use in computer programs for the simulation and modeling of real technological processes.

CONCLUSIONS

The conducted hot torsion tests for the selected grade of austenitic steel, performed under comparable experimental conditions at two research centers, revealed differences in the course of the plastic flow curves. The observed discrepancies concern both the level of flow stress values (σ_p) and the obtained values of limiting strain (ε_g) and the

strain corresponding to the maximum flow stress (ε_p). The variation in the flow curves results from both technical aspects of test execution, such as the method of specimen heating and the geometry of the gauge section, as well as from the calculation procedures used to determine strain based on the reduced radius of the specimen gauge section.

The presented experimental results and the analysis carried out at two independent research centers with well-established expertise in plastometric testing confirm the need to develop a standard for plastometric torsion testing. The proposed unified methodology for determining the characteristics of technological plasticity in the torsion test will systematize experimental procedures, from the selection of specimen geometry to the acquisition of test results. It will also standardize the method of converting recorded measurement data into flow stress and strain values. The application of a unified methodology will ensure repeatability and reproducibility of results in plastometric torsion testing. It is also expected to increase the use of torsion plastometry in metal processing industries for determining the strength properties of metal alloys and for real-time monitoring of metal forming processes.

Acknowledgements

Silesian University of Technology (Faculty of Materials Engineering), supported this work as a part of Statutory Research BK-220/RM1/2026 (11/010/BK_26/0061).

REFERENCES

1. Pawlicki J. Wpływ historii odkształcenia na naprężenie uplastyczniające w procesach odkształcania plastycznego na zimno. Wydawnictwo Politechniki Śląskiej; Monografia nr 369; Gliwice 2012.
2. Gabryszewski Z., Gronostajski J. Mechanika procesów obróbki plastycznej. PWN; Warszawa 1991.
3. Wang S., Dunlap A., Möhring K., Lohmar J., Schwedt A., Aretz A., Walther F., Hirt G. Torsion plastometer trials to investigate the effect of non-proportional loading paths in caliber rolling on damage and performance of metal parts. Production Engineering 2020; 14: 17–32, https://doi.org/10.1007/s11740-019-00949-5
4. Hojny M., Dębiński T., Głowacki M., Nguyen Trang T.T. Spatial thermo-mechanical model of mushy steel deformation based on the finite element method. Archives of Foundry Engineering. Polish Academy of Sciences. Commission of Foundry Engineering 2021; 21(2): 17–28. https://doi.org/10.24425/afe.2021.136093
5. Maciąg T., Migas D., Płachta A. Experimental confirmation of high-temperature phase boundaries in the nickel-rich part of Ni-Al-Cr system. Archives of Civil and Mechanical Engineering 2022; 22: 203. https://doi.org/10.1007/s43452-022-00532-3
6. Pantalé O., Muller Y., Balcaen Y. Advanced numerical modeling and experimental analysis of thermal gradients in Gleeble compression configuration for 2017-T4 aluminum alloy. Appl. Mech. 2024; 5: 839–855. https://doi.org/10.3390/applmech5040047
7. Wojtaszek M., Korpała G., Leboda T., Zyguła K., Prahl U. Hot processing of powder metallurgy and wrought ti-6al-4v alloy with large total deformation: physical modeling and verification by rolling. Metallurgical and Materials Transactions A 2020; 51: 5790–5805. https://doi.org/10.1007/s11661-020-05942-7
8. Jalme M.S, Desrayaud C., Favre J., Fabrègue D., Dancette S., Schuman C., Lecomte J.S., Archaud E., Dumont C. Microstructure evolution during multiaxial processing of TA6V. Materials Science Forum 2021; 1016: 1211–1217. https://doi.org/10.4028/www.scientific.net/MSF.1016.1211
9. Schindler I., Kawulok P.; Konečná, K., Sauer M., Navrátil H., Opěla, P., Kawulok, R. Rusz S. Simulation of hot continuous rolling of a plain carbon steel using the MaxStrain II® multiaxis deformation system. Arch. Metall. Mater. 2023; 68(2): 741–747. https://doi.org/10.24425/amm.2023.142456
10. Gronostajski Z. Modele konstytutywne opisujące zachowanie się wybranych stopów miedzi w zakresie dużych odkształceń plastycznych. Oficyna Wydawnicza Politechniki Wrocławskiej; Wrocław 2000.
11. Hadasik E. Metodyka wyznaczania charakterystyk plastyczności w próbie skręcania na gorąco. Zeszyty Naukowe Politechniki Śląskiej; z. 63: Gliwice 2002.
12. Grosman F., Hadasik E. Technologiczna plastyczność metali, badania plastometryczne. Wydawnictwo Politechniki Śląskiej; Gliwice 2005.
13. Kubina T., Boruta A., Longauerova M., Boruta J. Non-traditional use of torsion plastometer in physical simulation of steel production. Materials Science Forum 2014; 782: 51–56. https://doi.org/10.4028/www.scientific.net/MSF.782.51
14. Bressan J.D., Unfer R.K. Construction and validation tests of a torsion test machine, Journal of Materials Processing Technology 2006; 179: 23–29. https://doi.org/10.1016/j.jmatprotec.2006.03.099

15. Gembalova P., Boruta J., Grycz E., Cmiel K.M. Hot forming parameters research of bearing steel. Archives of Civil and Mechanical Engineering 2007; 7(2): 21–28. https://doi.org/10.1016/S1644-9665(12)60207-6
16. Laber K.B. Leszczyńska-Madej B. Theoretical and experimental analysis of the hot torsion process of the hardly deformable 5XXX series aluminium alloy. Materials 2021; 14(13): 3508. https://doi.org/10.3390/ma14133508
17. Gryc A., Bajor T., Dyja H., Sawicki S., Laber K. Physical modelling of plastic deformation conditions for the rolling process of AZ31 bars in a three high skew rolling mill. Metalurgija 2014; 53(4): 489–492.
18. Laber K., Kawałek A., Sawicki S., Dyja H., Borowski J., Leśniak D., Jurczak H. Application of torsion test for determination of rheological properties of 5019 aluminium alloy. Key Engineering Materials, Trans Tech Publications, Switzerland 2016; 682: 356–361. https://doi.org/10.4028/www.scientific.net/KEM.682.356
19. Gronostajski Z., Jaśkiewicz K. The effect of complex strain path on the properties of CuSi5 silicon bronze. Journal of Materials Processing Technology 2004; 155–156: 1144–1149. https://doi.org/10.1016/j.jmatprotec.2004.04.235
20. Funke P., Preiser H. Aufnahme von Fliesskurven im Warmverdrehversuch, Archiv für das Eisenhüttenwesen 1973; 5: 363–368.